

000 001 002 003 004 005 006 007 008 009 010 011 012 013 014 015 016 017 018 019 020 021 022 023 024 025 026 027 028 029 030 031 032 033 034 035 036 037 038 039 040 041 042 043 044 045 046 047 048 049 050 051 052 053 CROSS-MODEL DECEPTION: TRANSFERABLE ADVERSARIAL ATTACK FOR CODE SEARCH

Anonymous authors

Paper under double-blind review

ABSTRACT

Reliable code retrieval is crucial for developer productivity and effective code reuse, significantly impacting software engineering teams and organizations. However, the current neural code language models (CLMs) powering search tools are susceptible to adversarial attacks targeting non-functional textual elements. We introduce a language-agnostic transferable adversarial attack method that exploits this vulnerability of CLMs. Our approach perturbs identifiers within a code snippet without altering its functionality to deceptively align the code with a target query. In particular, we demonstrate that modifications based on smaller models, such as CodeT5+, are highly transferable to larger or closed-source models, like Nomic-emb-code or Voyage-code-3. These modifications can increase the similarity between the query and an arbitrary irrelevant code snippet, consequently degrading key retrieval metrics like Mean Reciprocal Rank (MRR) of the state-of-the-art models by up to 40%. The experimental results highlight the fragility of current code search methods and underscore the need for more robust, semantic-aware approaches. Our codebase is available at https://github.com/AdvAttackOnNCC/Code_Search_Adversarial_Attack.

1 INTRODUCTION

The rapid expansion of the computer science community coincides with an increased reliance on automated systems for code analysis. With public codebases growing in scale and complexity, the ability to efficiently understand, categorize, and retrieve code is critical (Shekhar, 2024). State-of-the-art models utilize neural networks to map code snippets into latent vector representations (i.e., embeddings) for various downstream tasks. Among these, code search aims to retrieve the most relevant code snippets for a given natural language query, promoting code reuse and boosting developer productivity (Di Grazia and Pradel, 2023; Sun et al., 2024; Li et al., 2025). These retrieval systems typically embed the query and code snippets into the same vector space in order to rank candidate snippets based on embedding similarity.

The advent of Large Language Models (LLMs) and specialized Code Language Models (CLMs) has enabled extensive improvements in code-related tasks such as code completion, summarization, and vulnerability detection, due to their advanced generation and reasoning capabilities (Jiang et al., 2024; Rozière et al., 2024; Hui et al., 2024; Chen et al., 2021). However, applying these large models directly to code search remains challenging (Howell et al., 2023), because the task typically involves retrieving relevant snippets from vast repositories containing thousands or even millions of candidates (Potvin and Levenberg, 2016). The large scale requires approaches that can both represent code compactly and perform efficient similarity-based ranking (Di Grazia and Pradel, 2023; Liu et al., 2021). Consequently, embedding-based retrieval models, which map code to vector spaces for efficient storage and similarity computation, are still essential for practical large-scale code search. Recent work indicates that employing these efficient embedding models through Retrieval-Augmented Generation (RAG) techniques allows LLMs to achieve more accurate and context-aware outputs for code generation tasks (Chen et al., 2024a; Wang et al., 2025a; Zhao et al., 2024).

Despite their utility, current neural code embedding models are vulnerable to adversarial examples—small, functionality-preserving modifications to code snippets that can drastically change their resulting embeddings (Chen et al., 2024b; Qu et al., 2024; Wan et al., 2022). While most prior research has focused on adversarial attacks in classification tasks (Yefet et al., 2020; Zhou et al., 2022;

Yao et al., 2024; Na et al., 2023), our work centers on code search, which leads to unique challenges. First, adversarial attacks in code search can be crafted to specific queries or retrieval contexts, allowing targeted manipulation of search results, for example pushing malicious cryptomining code to users with high computational resources. Second, the typical code search workflow introduces additional robustness issues. Unlike classification, where malicious code is processed directly during inference and can be potentially inspected by LLMs with reasoning abilities (Hort et al., 2025; Hossain et al., 2024; Jelodar et al., 2025), the code search is usually based on offline embedding. When large code corpora are embedded offline, the modified code snippets would appear harmless. Later, since the actual search process involves re-ranking based solely on these precomputed embeddings, it is much harder for LLMs or other systems to detect or mitigate these adversarial inputs.

In this paper, we demonstrate the shared vulnerability across CLMs through transferable adversarial attacks. The adversarial examples are initially generated by strategically replacing identifier tokens within a code snippet to maximize the embedding similarity between the modified code and a target query in small CLMs. We then highlight strong transferability: adversarial code snippets generated using one model remain consistently effective when embedded by other models across five tested programming languages. Notably, attacks crafted with a relatively small model (e.g., CodeT5+) can successfully deceive models that are 10 to 50 times larger (OASIS, Nomic-emb-code) or even closed-sourced (Voyage-code-3). Furthermore, the similarity changes the adversarial examples induce on the small source model strongly correlate with their effect on larger target models. In other words, the effectiveness of adversarial attacks on larger or closed-source models can be estimated efficiently on a smaller model, making these attacks more accessible.

Although state-of-the-art models report high scores on standard code search benchmarks (Li et al., 2024; Ott et al., 2022), they are vulnerable to our transferable adversarial attacks, which can cause dramatic drops in key retrieval metrics. For instance, we observed an absolute drop of 41-43% in Recall@1 across all tested models. The performance degradation suggests that high benchmark scores do not reflect code semantic understanding and further highlights the models’ reliance on brittle lexical features, indicating substantial room for improving their robustness. In summary, our contributions are as follows:

- We propose one of the first adversarial attack methods for code search, which perturbs the code snippet to maximize its similarity with the target query while preserving functionality;
- We illustrate transferability of the attack: adversarial code snippets generated using smaller models can effectively deceive larger models, including closed-source black-box systems; and
- We reveal that current state-of-the-art code search models rely on lexical features rather than deeper code understanding, exposing significant robustness gaps despite high benchmark performance and highlighting the need for future improvement.

2 RELATED WORKS

The field of Code Language Models (CLMs) has evolved rapidly, from early unified representations like CodeBERT (Feng et al., 2020) to encoder-decoders such as CodeT5 and CodeT5+ (Wang et al., 2021b; 2023). Subsequently, large generative CLMs, like Codex (Chen et al., 2021) and numerous open-source efforts, including CodeLlama (Rozière et al., 2024) and StarCoder (Li et al., 2023; Lozhkov et al., 2024), prominently showcase sophisticated code generation and reasoning abilities. The CLMs’ generative capabilities have been further enhanced by Retrieval-Augmented Generation (RAG) (Zhao et al., 2024). In RAG systems, CLMs leverage efficiently retrieved code snippets—often sourced via embedding models—to improve contextual relevance and accuracy for complex tasks (Wang et al., 2025b; Chen et al., 2024a; Wang et al., 2025a; Wu et al., 2024). The robustness of these underlying code embedding models is therefore critical, as the vulnerabilities explored in this paper directly threaten RAG pipelines and the corresponding CLM applications.

Code search, a crucial task for efficient software development and reuse (Nie et al., 2016), relies on embedding models for effective retrieval from large codebases. CodeSearchNet (Wu and Yan, 2022) established early benchmarks, with models like CodeBERT (Feng et al., 2020) learning joint natural language-code representations. To enhance understanding, later work incorporated structural information: GraphCodeBERT (Guo et al., 2020) used data flow graphs, while UniXcoder (Guo et al., 2022) and SynCoBERT (Wang et al., 2021a) leveraged Abstract Syntax Trees. Later, contrastive

learning, as seen in ContraCode (Jain et al., 2020), became a dominant training technique. Other strategies include adapting general CLM embeddings (Wang et al., 2023), fine-tuning LLMs (Nomic Team, 2025), or training on augmented data (Gao et al., 2025). Recently, black-box embedding services from OpenAI (OpenAI, 2024) and Voyage AI (Voyage AI, 2024) have also achieved state-of-the-art performance. However, our experimental results demonstrate that high benchmark scores do not guarantee robustness: top-performing code search models remain susceptible to the proposed adversarial attacks.

Applying gradient-based attack methods (Goodfellow et al., 2015) directly to natural language is challenging due to the discrete nature of the tokens, making it difficult to apply small perturbations while maintaining syntactic and semantic integrity (Zhang et al., 2020b). Programming languages, however, provide unique opportunities for adversarial attacks through semantic-preserving transformations (Hort et al., 2025). Attack strategies vary based on the assumed knowledge of the target model. White-box attacks require access to model gradients. Methods like DAMP (Yefet et al., 2020), MHM (Zhang et al., 2020a), and GraphCodeAttack (Nguyen et al., 2023) leverage gradient signals to guide modifications aiming for misclassification. Black-box attacks operate without internal model knowledge. CARL (Yao et al., 2024) utilizes reinforcement learning to optimize the attack, while ALERT (Yang et al., 2022) employs genetic algorithms and greedy search to find natural perturbations, and Wen et al. (2025) evaluates combinations of different search strategies. Other black-box methods based on heuristics include inserting comments or dead code (Na et al., 2023). Another emerging approach involves the use of generative models to directly produce adversarial code examples, as explored by CBA (Zhang et al., 2024) and ITGen (Huang et al., 2025). In this work, we propose a novel adversarial attack method in which we employ white-box attack techniques on one code search model to derive examples that also work as transferable black-box attacks against other models.

3 ADVERSARIAL ATTACK FOR CODE SEARCH

Inspired by the gradient-based optimization techniques in Yefet et al. (2020), previous gradient-based adversarial attack methods mainly focused on deceiving classification models by pushing the code snippet embedding to the category boundaries. Because code search systems can process both natural language queries and code snippets, our method is designed to increase the similarity between a code snippet and a target query. Our attack takes a *(query, code)* text pair, calculates their similarity score via the code search model, and uses the back-propagated gradient of this score on each token in the code snippet as the signal for the adversarial attack.

3.1 GRADIENT BASED METHOD

Formally, consider a query Q and an arbitrary code snippet C . Let Q_{emb} and C_{emb} represent their initial embeddings, typically derived from the embedding layer before any attention or subsequent processing within the code search model. We model the neural code search process with parameters θ as a function G_θ that maps these initial embeddings to a similarity score, $\text{Sim}_\theta(Q, C) = G_\theta(Q_{\text{emb}}, C_{\text{emb}})$. Our objective is to find a modified code snippet C' maximizing the similarity change:

$$\Delta \text{Sim}_\theta = \text{Sim}_\theta(Q, C') - \text{Sim}_\theta(Q, C) = G_\theta(Q_{\text{emb}}, C'_{\text{emb}}) - G_\theta(Q_{\text{emb}}, C_{\text{emb}}).$$

To search for optimal modifications efficiently, we approximate the similarity change using a first-order Taylor expansion. Let $C'_{\text{emb}} = C_{\text{emb}} + \delta$ be the initial embedding of the modified code, where δ represents the perturbation introduced by the token replacements. The similarity between the query and the modified code can be approximated as:

$$\begin{aligned} \text{Sim}_\theta(Q, C') &= G_\theta(Q_{\text{emb}}, C_{\text{emb}} + \delta) \approx G_\theta(Q_{\text{emb}}, C_{\text{emb}}) + \delta^\top \nabla_{C_{\text{emb}}} G_\theta(Q_{\text{emb}}, C_{\text{emb}}) \\ &= \text{Sim}_\theta(Q, C) + \delta^\top \nabla_{C_{\text{emb}}} G_\theta(Q_{\text{emb}}, C_{\text{emb}}) \end{aligned}$$

Therefore, maximizing the similarity change ΔSim_θ is approximately equivalent to maximizing the term $\delta^\top \nabla_{C_{\text{emb}}} G_\theta(Q_{\text{emb}}, C_{\text{emb}})$ that quantifies the impact of the embedding perturbation δ on the similarity score. We refer to this term as *influence* in the rest part of the paper.

Consider the specific case where a single token C_{t_i} at position i in the original code is replaced by a candidate token C_{t_x} . The perturbation vector $\delta_{(i, t_x)}$ will be zero everywhere except at the

162 dimensions corresponding to position i , where it equals the difference between the new and original
 163 token embeddings:

$$164 \quad \delta_{(i,t_x)} = (\vec{0}, \dots, \vec{0}, C_{\text{emb}_{t_x}} - C_{\text{emb}_{t_i}}, \vec{0}, \dots, \vec{0}).$$

166 To identify the best replacement for the token at position i , we calculate the expected change
 167 in similarity $\delta_{(i,t_x)}^\top \nabla_{C_{\text{emb}}} G_\theta(Q_{\text{emb}}, C_{\text{emb}})$ for every valid token C_{t_x} in the vocabulary. Since
 168 token replacements are happening at different positions, the search can be done concurrently: as
 169 $\delta_{(i,\cdot)} \cdot \delta_{(j,\cdot)} = 0$ for $i \neq j$.

$$170 \quad \max_{\delta} \delta^\top \nabla_{C_{\text{emb}}} G_\theta(Q_{\text{emb}}, C_{\text{emb}}) = \sum_i \max_{t_x} \delta_{(i,t_x)}^\top \nabla_{C_{\text{emb}}} G_\theta(Q_{\text{emb}}, C_{\text{emb}}).$$

173 To generate the adversarial code, tokens in the identifiers of C are replaced by iterating through the
 174 valid alternatives and selecting the tokens that maximize the influence. The resulting adversarial C'
 175 based on the query Q and code search model with parameter θ is denoted as $C' = \text{ADVATTACK}(Q, \theta)$.
 176 The examples of our adversarial attack method can be found in Appendix G.2.

177 At a high level, we preserve the code snippet’s functionality post-attack by enforcing two identifier
 178 renaming constraints:

- 180 • **Consistency:** All occurrences of the same identifier are replaced with the same new identifier.
- 181 • **Uniqueness:** Distinct identifiers are replaced with distinct new identifiers.

182 In practice, enforcing these constraints is more complex, because an identifier can consist of multiple
 183 tokens. The details of this approach are provided in Appendix E.

185 3.2 ATTACK TRANSFER

187 The gradient-based attack method requires access to the model parameters and sufficient compu-
 188 tational resources for the gradient back-propagation to the initial embedding of the code snippet.
 189 However, these prerequisites may not always be met, especially considering the increasing size of
 190 modern code search models and the rise of black-box code search systems.

191 For a code search model with parameter θ^* , which may be challenging to attack directly, our
 192 experimental results, presented in Section 4.2, demonstrate a practical alternative. We can generate
 193 an adversarial code snippet $C' = \text{ADVATTACK}(Q, \theta)$ using a smaller, more accessible model with
 194 parameter θ , and $\text{Sim}_{\theta^*}(Q, C') > \text{Sim}_{\theta^*}(Q, C)$ also holds with a very high probability. We refer to
 195 this phenomenon, where an attack crafted using one model is also effective on another, often more
 196 complex or inaccessible model, as “Attack Transfer.”

198 4 EXPERIMENTS AND RESULTS

200 This section presents the evaluation of our adversarial attack. First, we demonstrate the attack’s
 201 effectiveness on the sampled (*query, code*) pairs by quantifying the changes in the similarity scores and
 202 the number of pairs exhibiting similarity improvement (Section 4.1). Second, to assess transferability,
 203 we also report Precision, Pearson Correlation Coefficient (r), and Spearman’s Rank Correlation
 204 Coefficient (ρ), which measure the consistency of similarity changes across different model pairs
 205 (Section 4.2). Meanwhile, the effectiveness and the efficiency of the transferred attack are compared
 206 to the White-box and Black-box baselines (Section 4.3). Finally, we illustrate the attack’s practical
 207 impact on code search benchmarks and RAG systems by comparing standard metric scores before
 208 and after the attack (Section 4.4 and Section 4.5). The details of the metrics can be found in
 209 Appendix F.4. The collective results from our experiments show that the adversarial attack is effective
 210 and transferable across all datasets based on different programming languages and can substantially
 211 affect the retrieval performance of various models.

212 Our adversarial attack method can iteratively improve the code snippets’ similarity to the target query
 213 by reapplying the attack to their modified versions. In the experiments, the adversarial attack is
 214 performed for 5 iterations. The final adversarial code is then selected as that with maximum similarity
 215 across all candidates and the unperturbed original code. These design choices are discussed in the
 ablation studies in Appendix F.6.

216 Table 1: Models Used in the Experiments
217

Model	# Parameters	Vocabulary Size	# Tokens valid for identifiers
CodeT5+	110M	32103	29881
OASIS	1.54B	151665	74194
Nomic-embed-code	7.07B	151665	74194
Voyage-code-3	-	151665	74194

218 Table 2: Datasets Used in the Experiments
219

Dataset	# Queries	# Code Snippets	Programming Languages
CosQA	500	500	Python
CLARC	526	526	C++
HumanEval-X	164	164	Python, C++, Java, Javascript, Go

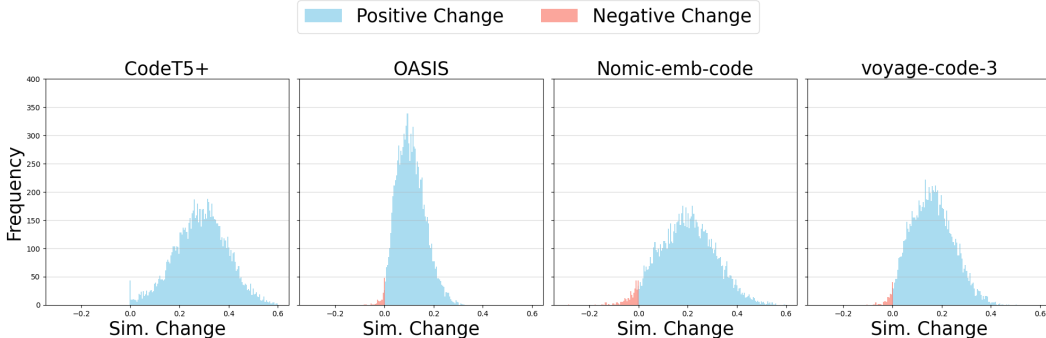
236 Figure 1: Distribution of Code Similarity Changes on CosQA. The Attack Model is CodeT5+, and
237 the Eval Models are labeled at the top of each subplot. The magnitude of negative similarity changes
238 resulting from the attack is considerably smaller than that of positive similarity changes.
239240 **Models** We applied a gradient-based adversarial attack to two models: CodeT5+ (Wang et al., 2023)
241 and OASIS (Gao et al., 2025). To assess the transferability of this attack, we evaluated the resulting
242 adversarial code examples on two additional models: Nomic-embed-code (Nomic Team, 2025)
243 and Voyage-code-3 (Voyage AI, 2024). Details regarding the models are provided in Table 1.244 **Datasets** We assessed the efficacy of our proposed adversarial attack using three datasets: CosQA
245 (Huang et al., 2021), CLARC (ClarcTeam, 2025), and HumanEval-X (Zheng et al., 2023), whose
246 statistics are detailed in Table 2. The code search benchmarks, CosQA and CLARC, were employed
247 to evaluate the effectiveness of the attack method and to quantify the impact of adversarial code on
248 retrieval metrics. Although HumanEval-X is not designed as a code search dataset, its shared queries
249 and code snippets with the same functionalities in five distinct programming languages allowed us to
250 conduct a controlled analysis of the attack across these different programming languages.
251252 4.1 EFFECTIVENESS OF THE ADVERSARIAL ATTACK
253254 To evaluate the effectiveness of our gradient-based adversarial attack, we constructed 20,000 (*query*,
255 *code*) pairs by sampling 100 queries and 100 code snippets from each of the CosQA (Huang et al.,
256 2021) and CLARC (ClarcTeam, 2025) datasets. Our attack method was applied to each pair to
257 generate the adversarial code.258 The highlighted rows in Table 3 present the effectiveness of our adversarial method on the 10,000
259 evaluation pairs from datasets. Our attack successfully increased the query-code similarity score in
260 over 97% of cases against the Attack Model. In the few remaining instances where no improvement
261 was observed, it was either because no token substitutions could be found that positively influenced the
262 similarity score or all possible substitutions led to decreased similarity. Since our method selects the
263 code version maximizing the similarity, in such cases, the original code is retained as the “adversarial”
264 code, resulting in zero change in similarity.265 It is also noteworthy that the scale of similarity change was larger on CodeT5+ compared to
266 OASIS. We hypothesize this is due to the denser embedding space of OASIS (as illustrated in
267 Appendix F.2), possibly stemming from its training on augmented data for robustness (Gao et al.,
268 2025). Furthermore, both the mean and standard error of the similarity changes were slightly higher
269 for the CosQA (Python) dataset compared to CLARC (C++), suggesting that programming languages
may influence the effectiveness of our gradient-based adversarial attack.

Table 3: Similarity Changes Resulting from Adversarial Attacks. Zero-change cases are classified as negative. **Highlighted rows** indicate settings where the Attack and Eval Models are the same. The similarity changes and the number of pairs with improved similarity demonstrate that the adversarial attack can effectively increase the similarity between a query and an arbitrary code snippet in most cases, even when the attack is not specifically targeting the Eval Model.

Dataset	Attack Model	Eval Model	Similarity Change (%)	Pos. Count	Positive Sim. Change (%)	Neg. Count	Negative Sim. Change (%)
CosQA	CodeT5+	CodeT5+	28.41 \pm 11.07	9908	28.67 \pm 10.78	92	0.00
		OASIS	10.59 \pm 5.81	9762	10.86 \pm 5.60	238	-0.65 \pm 1.36
		Nomic-emb-code	19.57 \pm 11.40	9539	20.63 \pm 10.55	461	-2.29 \pm 3.35
		Voyage-code-3	15.90 \pm 8.86	9808	16.23 \pm 8.40	192	-1.22 \pm 1.80
	OASIS	CodeT5+	10.74 \pm 11.85	8110	14.47 \pm 9.72	1890	-5.24 \pm 4.67
		OASIS	10.63 \pm 5.71	9814	10.84 \pm 5.58	186	0.00
		Nomic-emb-code	16.14 \pm 11.14	9321	17.48 \pm 10.29	679	-2.30 \pm 2.98
		Voyage-code-3	12.54 \pm 8.36	9580	13.13 \pm 8.04	420	-0.90 \pm 1.34
CLARC	CodeT5+	CodeT5+	24.84 \pm 8.62	9896	25.10 \pm 8.28	104	0.00
		OASIS	8.30 \pm 4.98	9540	8.77 \pm 4.57	460	-1.53 \pm 2.19
		Nomic-emb-code	14.01 \pm 8.38	9435	15.01 \pm 7.48	565	-2.65 \pm 3.72
		Voyage-code-3	9.01 \pm 5.73	9556	9.50 \pm 5.36	444	-1.59 \pm 2.24
	OASIS	CodeT5+	11.20 \pm 8.66	9080	12.73 \pm 7.47	920	-3.90 \pm 3.78
		OASIS	13.54 \pm 5.46	9789	13.83 \pm 5.14	211	0.00
		Nomic-emb-code	17.78 \pm 8.36	9675	18.42 \pm 7.73	325	-1.08 \pm 2.44
		Voyage-code-3	11.81 \pm 6.42	9732	12.15 \pm 6.17	268	-0.42 \pm 1.03

Table 4: Correlation in CosQA. r stands for Pearson Correlation Coefficient; ρ stands for Spearman’s Rank Correlation Coefficient. The high precision and correlation coefficients indicate that if an adversarial attack results in improved similarity on the Attack Model, a similarity improvement with a corresponding magnitude is also likely to be observed on the Eval Model.

Attack Model	Eval Model	Precision (%)	r (%)	ρ (%)
CodeT5+	OASIS	98.27	62.37	60.04
	Nomic-emb-code	96.14	62.47	60.14
	Voyage-code-3	98.48	64.13	62.17
OASIS	CodeT5+	81.56	63.35	63.75
	Nomic-emb-code	94.85	78.53	79.83
	Voyage-code-3	97.13	83.92	83.94

Table 5: Correlation in CLARC. The precision is comparable to CosQA, but the correlation coefficients are slightly lower. Although the scale of similarity change on both datasets are comparable, the lower correlation coefficients suggest that the attack transfer effects, while present, is less predictable or consistent on a case-by-case basis for CLARC than for CosQA.

Attack Model	Eval Model	Precision (%)	r (%)	ρ (%)
CodeT5+	OASIS	98.20	50.16	45.65
	Nomic-emb-code	95.16	49.68	45.43
	Voyage-code-3	96.21	46.39	42.61
OASIS	CodeT5+	91.35	48.21	46.46
	Nomic-emb-code	98.83	74.88	72.28
	Voyage-code-3	99.22	78.35	77.36

4.2 ATTACK TRANSFER

To assess the transferability of our adversarial attacks (introduced in Section 3.2), we used the same 20,000 (*query, code*) pairs sampled from the CosQA and CLARC datasets. Adversarial codes generated using CodeT5+ and OASIS (referred as “Attack Models”) were evaluated on different “Eval Models,” which computed embeddings and similarity scores for both the original and adversarial code snippets.

As shown in Tables 3, 4, and 5, our adversarial attacks exhibit strong cross-model transferability. Our results demonstrated consistent transferability of adversarial attacks across a diverse set of Eval Models, including compact models (CodeT5+), robustness-enhanced models (OASIS), models fine-tuned from large CLMs (Nomic-emb-code), and closed-source systems (Voyage-code-3). For most Attack/Eval Model pairs, over 95% of adversarial examples successfully increased query-code similarity scores on the Eval Model. Precision—the probability that an adversarial example induces a positive similarity change on the Eval Model when it did so on the Attack Model—typically exceeded 90–95%. Moreover, we observed moderate to strong positive Pearson (r) and Spearman (ρ) correlations, indicating that adversarial examples causing larger similarity increases on the Attack Model tend to yield similarly large gains on the Eval Models. Although a minority of adversarial

324
 325 Table 6: Comparison of the Attack Transfer against baselines. In the white-box scenario, the attack
 326 achieves performance comparable to the baseline while using only $\sim 60\%$ of the GPU hours. In the
 327 black-box scenario, our attack transfer is more effective and requires just 0.01% of the API calls used
 328 by CodeAttack. GPU hours are calculated on a Nvidia L40 ADA 48GB GPU.

Method	Similarity Change (%)	Pos. Count	Positive Sim. Change (%)	Neg. Count	Negative Sim. Change (%)	Efficiency
White Box	Direct Attack	10.45 \pm 5.48	978	10.69 \pm 5.31	22	0.00 \pm 0.00
	Attack Transfer	10.29 \pm 5.76	985	10.46 \pm 5.63	15	4.61 \pm 1.89
Black Box	CodeAttack	5.18 \pm 4.18	907	5.95 \pm 3.54	93	-0.02 \pm 2.10
	Attack Transfer	15.81 \pm 8.79	969	16.36 \pm 8.35	30	-1.56 \pm 1.76

335
 336 examples led to a decrease in similarity (see Figure 1 and Appendix F.1), the magnitude of these
 337 decreases was generally much smaller than the gains from successful transfers.

338
 339 Interestingly, differences in tokenization between the Attack and Eval Models did not hinder trans-
 340 ferability. Our method relies on the Attack Model’s vocabulary for token substitutions. Although
 341 CodeT5+ uses a tokenizer with only one-fifth the vocabulary size of `Nomic-emb-code` and
 342 `Voyage-code-3`, its adversarial examples still transferred effectively, achieving performance
 343 comparable to those generated by `OASIS`, whose tokenizer is nearly identical to the two Eval Models.

344
 345 We also observed an asymmetry in transferability. Attacks generated by CodeT5+ transferred
 346 well to `OASIS`, with high precision, whereas `OASIS` attacks transferred less effectively to
 347 CodeT5+, showing lower precision and weaker correlation. When targeting `Nomic-emb-code`
 348 and `Voyage-code-3`, CodeT5+ and `OASIS` attacks produced comparable similarity changes, but
 349 `OASIS` attacks consistently achieved higher correlation coefficients, which suggests that `OASIS` may
 350 exploit features more aligned with those captured by `Nomic-emb-code` and `Voyage-code-3`,
 351 potentially due to similarities in architecture, parameter size, or tokenization.

352 4.3 COMPARISON WITH BASELINES

353
 354 We also evaluated our Attack Transfer method against corresponding baselines in both white-box
 355 and black-box settings, using 1,000 (*query, code*) pairs from the CosQA dataset. For the white-box
 356 scenario, we compared a transferred attack from CodeT5+ to `OASIS` against a baseline direct attack
 357 based on the `OASIS` model. As our work is among the first to explore adversarial attacks on code
 358 search, we define the white-box baseline as a direct attack where the attack and evaluation models are
 359 identical. For the black-box scenario, our transferred attack from CodeT5+ to `Voyage-code-3`
 360 was compared against applying adapted CodeAttack (Jha and Reddy, 2023)¹ to `Voyage-code-3`.

361
 362 The comparison results are presented in Table 6. In the white-box setting, our attack transfer achieves
 363 performance comparable to the direct attack but with better efficiency, requiring $\sim 40\%$ less GPU
 364 time. The advantages of our method are even more pronounced in the black-box comparison. Attack
 365 transfer is not only substantially more effective than CodeAttack but also orders of magnitude more
 366 efficient, using a tiny fraction of the API calls. Moreover, our method preserves the functionality of
 367 the code, whereas modifications by CodeAttack often produce non-compilable code snippets.

368 4.4 APPLICATION ON CODE SEARCH BENCHMARKS

369
 370 In this experiment, CodeT5+ was used as the Attack Model. For each query in the CosQA and
 371 CLARC datasets, we selected 10% of irrelevant code snippets and modified them adversarially to max-
 372 imize their similarity to the query. These modified snippets replaced the original irrelevant ones in the
 373 candidate pools. Eval Models (CodeT5+, `OASIS`, `Nomic-emb-code`, and `Voyage-code-3`)
 374 then embedded the queries and the modified pools and reranked the code snippets by similarity. The
 375 retrieval metrics are measured before and after this replacement.

376
 377 ¹CodeAttack was originally developed for the code classification task, and we modified it to fit our code
 378 search objective.

378
 379
 380
 381
 382
 383 Table 7: Code Search Metric Change Caused by 10% Adversarial Attack on CosQA. The statistics
 384 reveal a consistent degradation in all metrics for every code search model after the attack, underscoring
 385 the adversarial attack’s substantial influence on their retrieval capability. The metric changes when
 386 other percentages of the corpus are attacked are available in Appendix F.5.
 387
 388
 389
 390
 391
 392
 393

Model	Setting	MRR	NDCG	Recall@1	Recall@5	Recall@10	Recall@20
CodeT5+ (Attack Model)	Original	74.08	78.52	64.00	88.20	92.20	95.20
	Adversarial	11.81	15.19	7.20	18.20	26.40	36.40
	Δ	62.27	63.33	56.80	70.00	65.80	58.80
OASIS	Original	80.27	84.51	70.40	92.80	97.60	99.60
	Adversarial	40.63	48.09	28.40	56.60	72.20	85.00
	Δ	39.64	36.42	42.00	36.20	25.40	14.60
Nomic-emb-code	Original	82.83	86.40	73.40	94.40	97.20	98.60
	Adversarial	42.81	49.74	30.00	59.60	71.80	82.80
	Δ	40.01	36.66	43.40	34.80	25.40	15.80
Voyage-code-3	Original	87.03	89.84	79.40	96.80	98.20	99.20
	Adversarial	50.94	57.92	38.00	69.80	80.00	90.60
	Δ	36.09	31.92	41.40	27.00	18.20	8.60

394
 395 As shown in Table 7, replacing only 10% of irrelevant candidates with adversarial versions led to
 396 sharp performance drops in all models. Before attack, models like OASIS, Nomic-emb-code, and
 397 Voyage-code-3 achieved strong R@1 (70-80%) and R@5 (>90%) scores, suggesting the task
 398 was nearly “solved.” However, after attack, R@1 fell by over 40%, and R@5 dropped below 70%,
 399 revealing that high benchmark scores do not guarantee robustness against adversarial manipulation.
 400

401 Unsurprisingly, CodeT5+, the Attack Model, had the greatest performance drop. Yet the attack also
 402 transferred effectively to other models. OASIS remained vulnerable, despite being trained against
 403 hard negatives with similar keywords on an augmented dataset. Nomic-emb-code’s substantial
 404 performance decrease (R@1 decreased by >43%) indicates even large CLMs can overly depend on
 405 lexical features like identifiers, suggesting that scale-up does not naturally yield greater robustness.
 406 Although Voyage-code-3 was the most resilient, it still suffered a notable performance drop,
 407 confirming the attack’s potent transferability even against closed-source systems.
 408

4.5 APPLICATION ON RAG SYSTEMS

409 To demonstrate how adversarial attacks on a code corpus can
 410 impact downstream RAG systems, we also evaluated the per-
 411 formance of a system based on `gpt-4o` on the HumanEval bench-
 412 mark, following the pipeline from CodeRAG-Bench (Wang
 413 et al., 2025b). We measured the Pass@1 under three scenar-
 414 ios: **Standard RAG**, which uses retrieval from the original
 415 corpus; **Gold Retrieval**, which uses ground-truth code snippets
 416 to establish an upper-bound performance; and **Attacked RAG**,
 417 which uses retrieval from a corpus where 10% of the code is
 418 adversarially modified.

419 The experimental results, presented in Table 8, show a notable
 420 drop in performance for the **Attacked RAG** scenario. The
 421 degradation highlights that for a RAG system that employs a
 422 highly capable generator model, its overall performance can be
 423 undermined if the underlying retrieval component is com-
 424 promised by an attack.

4.6 PROGRAMMING LANGUAGES

425 To assess the effectiveness of attack transfer across languages, we used the HumanEval-X
 426 dataset (Zheng et al., 2023), which includes 164 queries with solutions in Python, C++, Java,
 427 JavaScript, and Go. We created 26,732 (*query, code*) pairs by pairing each query with all non-
 428 corresponding solutions. CodeT5+ served as the Attack Model, while OASIS, Nomic-emb-code,
 429 and Voyage-code-3 were used as Eval Models.

430
 431 Table 8: Performance of Code RAG
 432 System based on GPT-4o on Hu-
 433 manEval. The lower Pass@1 in
 434 the **bold** row demonstrated the in-
 435 fluence of the adversarial attack
 436 on the code RAG system. Re-
 437 sults marked with an asterisk (*)
 438 are from CodeRAG-Bench (Wang
 439 et al., 2025b).

Method	Pass@1
Standard RAG	90.9%
Gold Retrieval	92.6%*
Attacked RAG	87.2%

432 Table 9: Effectiveness and Correlation of Adversarial Attack transferred from CodeT5+ in Various
 433 Programming Languages in HumanEval-X. “Positive” indicates the percentage of 26,732 pairs with
 434 increased similarity after the attack; “Negative” indicates the percentage with decreased or unchanged
 435 similarity. The similarity changes and the ratio of positive similarity changes confirm the effectiveness
 436 of the adversarial attack across all 5 programming languages.

Eval Model	Similarity Change (%)	Positive (%)	Pos. Sim. Change (%)	Negative (%)	Neg. Sim. Change (%)	Precision (%)	r (%)	ρ (%)
Python								
CodeT5+	22.49	97.9	23.05	2.1	0	-	-	-
OASIS	6.72	96.1	7.06	3.9	-0.91	97.12	53.39	50.49
Nomic-code-emb	11.52	91.7	12.88	8.3	-2.60	93.37	49.54	46.88
Voyage-code-3	5.92	96.2	6.20	3.8	-0.69	97.36	46.09	42.80
C++								
CodeT5+	18.72	99.2	18.86	0.8	0	-	-	-
OASIS	5.96	90.1	6.85	9.9	-2.09	90.55	50.40	49.46
Nomic-code-emb	7.56	81.3	10.28	18.7	-4.33	81.91	46.32	45.37
Voyage-code-3	6.20	92.9	6.81	7.1	-1.74	93.16	39.59	38.12
Java								
CodeT5+	17.26	99.2	17.40	0.8	0	-	-	-
OASIS	6.25	90.8	7.08	9.2	-1.99	91.28	48.46	47.48
Nomic-code-emb	8.26	82.5	10.91	17.5	-4.23	83.10	44.25	42.97
Voyage-code-3	7.57	95.8	7.97	4.2	-1.57	96.30	43.52	42.12
JavaScript								
CodeT5+	20.61	99.4	20.73	0.6	0	-	-	-
OASIS	7.02	91.0	7.96	9.0	-2.42	91.28	52.01	50.40
Nomic-code-emb	11.05	87.3	13.34	12.7	-4.66	87.72	48.46	46.30
Voyage-code-3	8.04	92.0	8.94	8.0	-2.30	92.31	45.05	43.41
Go								
CodeT5+	22.95	99.8	23.00	0.2	0	-	-	-
OASIS	8.27	94.4	8.90	5.6	-2.35	94.56	51.68	49.69
Nomic-code-emb	11.07	88.6	13.07	11.4	-4.42	88.76	48.20	45.94
Voyage-code-3	8.13	94.8	8.69	5.2	-2.04	94.90	42.56	40.19

460 As shown in Table 9, the adversarial attack was effective and transferable across all five languages,
 461 with varied impact. Python and Go experienced the largest similarity changes, while C++, Java, and
 462 JavaScript were less affected. Transferability was stronger for languages with flexible structures. Go
 463 achieved the highest similarity change, and Python had the highest transfer precision. Conversely,
 464 the statically typed C++ and Java showed slightly weaker transferability, especially when targeting
 465 Nomic-emb-code.

466 Despite these variations, correlation coefficients were consistent across languages, suggesting that the
 467 linear or monotonic correlation between the attack’s impact on the Attack Model and its transferred
 468 impact on Eval Models is stable regardless of language. In general, adversarial code snippets that
 469 cause greater similarity changes on the Attack Model are expected to be similarly effective on Eval
 470 Models, irrespective of the specific programming language.

472 5 CONCLUSION & FUTURE WORKS

474 We propose a transferable adversarial attack that modifies code identifiers to mislead code search
 475 models. The attack transfer is highly effective across a range of models, demonstrating current
 476 models’ reliance on superficial features. The revealed vulnerability underscores the urgent need for
 477 more robust and semantics-aware code embedding techniques.

478 Future research could explore several directions. First, the strong correlation in attack transferability
 479 across models warrants further investigation into shared pre-training data or common architectural
 480 biases. Second, future work could focus on developing more robust code embedding models through
 481 new defense mechanisms or training strategies, such as contrastive learning tailored to functionality-
 482 preserving perturbations. Lastly, because the attack exploits the difference between natural and
 483 programming languages, simply adapting NLP procedures for CLMs may be inadequate, especially
 484 when fine-tuning data might be insufficient to address the unique scenario. Instead, integrating
 485 programming language-specific structures, such as Abstract Syntax Trees, could be a more efficient
 approach toward building more robust and semantically grounded CLMs.

486 REPRODUCIBILITY STATEMENT
487

488 The authors confirm that the code and data required to reproduce the experimental re-
489 sults presented in Section 4 are publicly available. The codebase is hosted on GitHub at
490 https://github.com/AdvAttackOnNCC/Code_Search_Adversarial_Attack,
491 and the dataset is available on Hugging Face at <https://huggingface.co/datasets/CoIR-Retrieval/cosqa>,
492 <https://huggingface.co/datasets/ClarcTeam/CLARC>, and <https://github.com/zai-org/CodeGeeX?tab=readme-ov-file#humaneval-x-a-new-benchmark-for-multilingual-program-synthesis>. All
493 results were verified to be reproducible with our implementation as of the submission date (September
494 22, 2025). We note the specific date as certain experimental results rely on API calls (gpt-4o,
495 Voyage-code-3).
496
497

498 REFERENCES
499

500 Junkai Chen, Xing Hu, Zhenhao Li, Cuiyun Gao, Xin Xia, and David Lo. Code search is all
501 you need? improving code suggestions with code search. In *Proceedings of the IEEE/ACM
502 46th International Conference on Software Engineering*, ICSE '24, New York, NY, USA, 2024a.
503 Association for Computing Machinery. ISBN 9798400702174. doi: 10.1145/3597503.3639085.
504 URL <https://doi.org/10.1145/3597503.3639085>.
505

506 Mark Chen, Jerry Tworek, Heewoo Jun, Qiming Yuan, Henrique Ponde de Oliveira Pinto, Jared Ka-
507 plan, Harri Edwards, Yuri Burda, Nicholas Joseph, Greg Brockman, Alex Ray, Raul Puri, Gretchen
508 Krueger, Michael Petrov, Heidy Khlaaf, Girish Sastry, Pamela Mishkin, Brooke Chan, Scott Gray,
509 Nick Ryder, Mikhail Pavlov, Alethea Power, Lukasz Kaiser, Mohammad Bavarian, Clemens
510 Winter, Philippe Tillet, Felipe Petroski Such, Dave Cummings, Matthias Plappert, Fotios Chantzis,
511 Elizabeth Barnes, Ariel Herbert-Voss, William Hebgen Guss, Alex Nichol, Alex Paino, Nikolas
512 Tezak, Jie Tang, Igor Babuschkin, Suchir Balaji, Shantanu Jain, William Saunders, Christopher
513 Hesse, Andrew N. Carr, Jan Leike, Josh Achiam, Vedant Misra, Evan Morikawa, Alec Radford,
514 Matthew Knight, Miles Brundage, Mira Murati, Katie Mayer, Peter Welinder, Bob McGrew, Dario
515 Amodei, Sam McCandlish, Ilya Sutskever, and Wojciech Zaremba. Evaluating large language
models trained on code, 2021. URL <https://arxiv.org/abs/2107.03374>.
516

517 Yuchen Chen, Weisong Sun, Chunrong Fang, Zhenpeng Chen, Yifei Ge, Tingxu Han, Quanjun Zhang,
518 Yang Liu, Zhenyu Chen, and Baowen Xu. Security of language models for code: A systematic
519 literature review. *arXiv preprint arXiv:2410.15631*, 2024b.

520 ClarcTeam. CLARC Dataset. <https://huggingface.co/datasets/ClarcTeam/CLARC>, 2025. Accessed: 2025-05-07.
521
522

523 Luca Di Grazia and Michael Pradel. Code search: A survey of techniques for finding code. *ACM
524 Computing Surveys*, 55(11):1–31, 2023.

525 Zhangyin Feng, Daya Guo, Duyu Tang, Nan Duan, Xiaocheng Feng, Ming Gong, Linjun Shou, Bing
526 Qin, Ting Liu, Dixin Jiang, and Ming Zhou. Codebert: A pre-trained model for programming and
527 natural languages, 2020. URL <https://arxiv.org/abs/2002.08155>.
528

529 Zuchen Gao, Zizheng Zhan, Xianming Li, Erxin Yu, Ziqi Zhan, Haotian Zhang, Bin Chen, Yuqun
530 Zhang, and Jing Li. Oasis: Order-augmented strategy for improved code search. *arXiv preprint
531 arXiv:2503.08161*, 2025.

532 Ian J. Goodfellow, Jonathon Shlens, and Christian Szegedy. Explaining and harnessing adversarial
533 examples, 2015. URL <https://arxiv.org/abs/1412.6572>.
534

535 Daya Guo, Shuo Ren, Shuai Lu, Zhangyin Feng, Duyu Tang, Shujie Liu, Long Zhou, Nan Duan,
536 Alexey Svyatkovskiy, Shengyu Fu, et al. Graphcodebert: Pre-training code representations with
537 data flow. *arXiv preprint arXiv:2009.08366*, 2020.

538 539 Daya Guo, Shuai Lu, Nan Duan, Yanlin Wang, Ming Zhou, and Jian Yin. Unixcoder: Unified
cross-modal pre-training for code representation. *arXiv preprint arXiv:2203.03850*, 2022.

540 Max Hort, Linas Vidziunas, and Leon Moonen. Semantic-preserving transformations as mutation
 541 operators: A study on their effectiveness in defect detection. In *2025 IEEE International Conference*
 542 *on Software Testing, Verification and Validation Workshops (ICSTW)*, pages 337–346. IEEE, 2025.

543

544 Al Amin Hossain, Mithun Kumar PK, Junjie Zhang, and Fathi Amsaad. Malicious code detection
 545 using llm. In *NAECON 2024 - IEEE National Aerospace and Electronics Conference*, pages
 546 414–416, 2024. doi: 10.1109/NAECON61878.2024.10670668.

547 Kristen Howell, Gwen Christian, Pavel Fomitchov, Gittit Kehat, Julianne Marzulla, Leanne Rolston,
 548 Jadin Tredup, Ilana Zimmerman, Ethan Selfridge, and Joseph Bradley. The economic trade-offs of
 549 large language models: A case study. *arXiv preprint arXiv:2306.07402*, 2023.

550

551 Junjie Huang, Duyu Tang, Linjun Shou, Ming Gong, Ke Xu, Dixin Jiang, Ming Zhou, and Nan
 552 Duan. CoSQA: 20,000+ web queries for code search and question answering. In Chengqing
 553 Zong, Fei Xia, Wenjie Li, and Roberto Navigli, editors, *Proceedings of the 59th Annual Meeting*
 554 *of the Association for Computational Linguistics and the 11th International Joint Conference*
 555 *on Natural Language Processing (Volume 1: Long Papers)*, pages 5690–5700, Online, August
 556 2021. Association for Computational Linguistics. doi: 10.18653/v1/2021.acl-long.442. URL
 557 <https://aclanthology.org/2021.acl-long.442/>.

558

559 Li Huang, Weifeng Sun, and Meng Yan. Iterative Generation of Adversarial Example for Deep
 560 Code Models . In *2025 IEEE/ACM 47th International Conference on Software Engineering*
 561 (*ICSE*), pages 623–623, Los Alamitos, CA, USA, May 2025. IEEE Computer Society. doi:
 562 10.1109/ICSE55347.2025.00086. URL <https://doi.ieee.org/10.1109/ICSE55347.2025.00086>.

563

564 Binyuan Hui, Jian Yang, Zeyu Cui, Jiaxi Yang, Dayiheng Liu, Lei Zhang, Tianyu Liu, Jiajun Zhang,
 565 Bowen Yu, Kai Dang, et al. Qwen2. 5-coder technical report. *arXiv preprint arXiv:2409.12186*,
 566 2024.

567

568 Paras Jain, Ajay Jain, Tianjun Zhang, Pieter Abbeel, Joseph E Gonzalez, and Ion Stoica. Contrastive
 569 code representation learning. *arXiv preprint arXiv:2007.04973*, 2020.

570

571 Hamed Jelodar, Samita Bai, Parisa Hamed, Hesamoddin Mohammadian, Roozbeh Razavi-Far, and
 572 Ali Ghorbani. Large language model (llm) for software security: Code analysis, malware analysis,
 573 reverse engineering, 2025. URL <https://arxiv.org/abs/2504.07137>.

574

575 Akshita Jha and Chandan K. Reddy. Codeattack: code-based adversarial attacks for pre-trained pro-
 576 gramming language models. In *Proceedings of the Thirty-Seventh AAAI Conference on Artificial In-
 577 telligence and Thirty-Fifth Conference on Innovative Applications of Artificial Intelligence and Thir-
 578 teenth Symposium on Educational Advances in Artificial Intelligence, AAAI’23/IAAI’23/EAAI’23*.
 579 AAAI Press, 2023. ISBN 978-1-57735-880-0. doi: 10.1609/aaai.v37i12.26739. URL <https://doi.org/10.1609/aaai.v37i12.26739>.

580

581 Juyong Jiang, Fan Wang, Jiasi Shen, Sungju Kim, and Sunghun Kim. A survey on large language
 582 models for code generation, 2024. URL <https://arxiv.org/abs/2406.00515>.

583

584 Harold W. Kuhn. The hungarian method for the assignment problem. *Naval Research Logistics*
 585 *Quarterly*, 2(1-2):83–97, 1955. doi: 10.1002/nav.3800020109.

586

587 Raymond Li, Loubna Ben Allal, Yangtian Zi, Niklas Muennighoff, Denis Kocetkov, Chenghao Mou,
 588 Marc Marone, Christopher Akiki, Jia Li, Jenny Chim, et al. Starcoder: may the source be with
 589 you! *arXiv preprint arXiv:2305.06161*, 2023.

590

591 Xiangyang Li, Kuicai Dong, Yi Quan Lee, Wei Xia, Hao Zhang, Xinyi Dai, Yasheng Wang, and Ruim-
 592 ing Tang. Coir: Compressed object-oriented image representation. <https://archersama.github.io/coir/>, 2024. Accessed: 2024-09-24. Author and year not explicitly stated on the
 593 webpage.

594

595 Xiangyang Li, Kuicai Dong, Yi Quan Lee, Wei Xia, Hao Zhang, Xinyi Dai, Yasheng Wang, and
 596 Ruiming Tang. CoIR: A comprehensive benchmark for code information retrieval models. In
 597 Wanxiang Che, Joyce Nabende, Ekaterina Shutova, and Mohammad Taher Pilehvar, editors,
 598 *Proceedings of the 63rd Annual Meeting of the Association for Computational Linguistics (Volume*

594 *1: Long Papers*), pages 22074–22091, Vienna, Austria, July 2025. Association for Computational
 595 Linguistics. ISBN 979-8-89176-251-0. doi: 10.18653/v1/2025.acl-long.1072. URL <https://aclanthology.org/2025.acl-long.1072/>.

596

597 Chao Liu, Xin Xia, David Lo, Cuiyun Gao, Xiaohu Yang, and John Grundy. Opportunities and
 598 challenges in code search tools. *ACM Comput. Surv.*, 54(9), October 2021. ISSN 0360-0300. doi:
 599 10.1145/3480027. URL <https://doi.org/10.1145/3480027>.

600

601 Anton Lozhkov, Raymond Li, Loubna Ben Allal, Federico Cassano, Joel Lamy-Poirier, Nouamane
 602 Tazi, Ao Tang, Dmytro Pykhtar, Jiawei Liu, Yuxiang Wei, et al. Starcoder 2 and the stack v2: The
 603 next generation. *arXiv preprint arXiv:2402.19173*, 2024.

604

605 CheolWon Na, YunSeok Choi, and Jee-Hyong Lee. DIP: Dead code insertion based black-
 606 box attack for programming language model. In Anna Rogers, Jordan Boyd-Graber, and
 607 Naoaki Okazaki, editors, *Proceedings of the 61st Annual Meeting of the Association for Com-
 608 putational Linguistics (Volume 1: Long Papers)*, pages 7777–7791, Toronto, Canada, July
 609 2023. Association for Computational Linguistics. doi: 10.18653/v1/2023.acl-long.430. URL
 610 <https://aclanthology.org/2023.acl-long.430/>.

611 Thanh-Dat Nguyen, Yang Zhou, Xuan Bach D Le, Patanamon Thongtanunam, and David Lo. Adver-
 612 sarial attacks on code models with discriminative graph patterns. *arXiv preprint arXiv:2308.11161*,
 613 2023.

614 Liming Nie, He Jiang, Zhilei Ren, Zeyi Sun, and Xiaochen Li. Query expansion based on crowd
 615 knowledge for code search. *IEEE Transactions on Services Computing*, 9(5):771–783, September
 616 2016. ISSN 1939-1374. doi: 10.1109/tsc.2016.2560165. URL <http://dx.doi.org/10.1109/TSC.2016.2560165>.

617

618 Nomic Team. Nomic Embed Code: A State-of-the-Art Code Retriever. <https://www.nomic.ai/blog/posts/introducing-state-of-the-art-nomic-embed-code>, 2025.
 619 Nomic Blog; accessed May 5, 2025.

620

621 OpenAI. New embedding models and api updates, January 2024. URL <https://openai.com/index/new-embedding-models-and-api-updates/>.

622

623 Simon Ott, Adriano Barbosa-Silva, Kathrin Blagec, Jan Brauner, and Matthias Samwald. Map-
 624 ping global dynamics of benchmark creation and saturation in artificial intelligence. *Nature
 625 Communications*, 13(1):6793, 2022.

626

627 Rachel Potvin and Josh Levenberg. Why google stores billions of lines of code in a single repository.
 628 *Communications of the ACM*, 59:78–87, 2016. URL <http://dl.acm.org/citation.cfm?id=2854146>.

629

630 Yubin Qu, Song Huang, and Yongming Yao. A survey on robustness attacks for deep code models.
 631 *Automated Software Engineering*, 31(2):65, 2024.

632

633 Baptiste Rozière, Jonas Gehring, Fabian Gloeckle, Sten Sootla, Itai Gat, Xiaoqing Ellen Tan, Yossi
 634 Adi, Jingyu Liu, Romain Sauvestre, Tal Remez, Jérémie Rapin, Artyom Kozhevnikov, Ivan Evtimov,
 635 Joanna Bitton, Manish Bhatt, Cristian Canton Ferrer, Aaron Grattafiori, Wenhan Xiong, Alexandre
 636 Défosséz, Jade Copet, Faisal Azhar, Hugo Touvron, Louis Martin, Nicolas Usunier, Thomas
 637 Scialom, and Gabriel Synnaeve. Code llama: Open foundation models for code, 2024. URL
 638 <https://arxiv.org/abs/2308.12950>.

639

640 Gaurav Shekhar. The impact of ai and automation on software
 641 development: A deep dive. <https://ieeechicago.org/the-impact-of-ai-and-automation-on-software-development-a-deep-dive/>,
 642 November 2024. IEEE Chicago Section. Accessed 2025-05-01.

643

644 Weisong Sun, Chunrong Fang, Yifei Ge, Yuling Hu, Yuchen Chen, Quanjun Zhang, Xiuting Ge,
 645 Yang Liu, and Zhenyu Chen. A survey of source code search: A 3-dimensional perspective. *ACM
 646 Trans. Softw. Eng. Methodol.*, 33(6), June 2024. ISSN 1049-331X. doi: 10.1145/3656341. URL
 647 <https://doi.org/10.1145/3656341>.

648 Voyage AI. *voyage-code-3: more accurate code retrieval with lower dimensional, quantized embed-*
 649 *dings*, December 2024.

650

651 Yao Wan, Shijie Zhang, Hongyu Zhang, Yulei Sui, Guandong Xu, Dezhong Yao, Hai Jin, and
 652 Lichao Sun. You see what i want you to see: poisoning vulnerabilities in neural code search. In
 653 *Proceedings of the 30th ACM Joint European Software Engineering Conference and Symposium*
 654 *on the Foundations of Software Engineering*, ESEC/FSE 2022, page 1233–1245, New York, NY,
 655 USA, 2022. Association for Computing Machinery. ISBN 9781450394130. doi: 10.1145/3540250.
 656 3549153. URL <https://doi.org/10.1145/3540250.3549153>.

657

658 Xin Wang, Yasheng Wang, Fei Mi, Pingyi Zhou, Yao Wan, Xiao Liu, Li Li, Hao Wu, Jin Liu, and
 659 Xin Jiang. Syncobert: Syntax-guided multi-modal contrastive pre-training for code representation.
 660 *arXiv preprint arXiv:2108.04556*, 2021a.

661

662 Yuchen Wang, Shangxin Guo, and Chee Wei Tan. From code generation to software testing: Ai
 663 copilot with context-based rag. *IEEE Software*, pages 1–9, 2025a. doi: 10.1109/MS.2025.3549628.

664

665 Yue Wang, Weishi Wang, Shafiq Joty, and Steven C. H. Hoi. Codet5: Identifier-aware unified
 666 pre-trained encoder-decoder models for code understanding and generation, 2021b. URL <https://arxiv.org/abs/2109.00859>.

667

668 Yue Wang, Hung Le, Akhilesh Deepak Gotmare, Nghi DQ Bui, Junnan Li, and Steven CH Hoi.
 669 Codet5+: Open code large language models for code understanding and generation. *arXiv preprint*
 670 *arXiv:2305.07922*, 2023.

671

672 Zora Zhiruo Wang, Akari Asai, Xinyan Velocity Yu, Frank F. Xu, Yiqing Xie, Graham Neubig, and
 673 Daniel Fried. CodeRAG-bench: Can retrieval augment code generation? In Luis Chiruzzo, Alan
 674 Ritter, and Lu Wang, editors, *Findings of the Association for Computational Linguistics: NAACL*
 675 2025, pages 3199–3214, Albuquerque, New Mexico, April 2025b. Association for Computational
 676 Linguistics. ISBN 979-8-89176-195-7. doi: 10.18653/v1/2025.findings-naacl.176. URL [https://aclanthology.org/2025.findings-naacl.176/](https://aclanthology.org/2025.findings-naacl.176).

677

678 Jin Wen, Qiang Hu, Yuejun Guo, Maxime Cordy, and Yves Le Traon. Variable renaming-based
 679 adversarial test generation for code model: Benchmark and enhancement. *ACM Trans. Softw. Eng.*
 680 *Methodol.*, March 2025. ISSN 1049-331X. doi: 10.1145/3723353. URL <https://doi.org/10.1145/3723353>. Just Accepted.

681

682 Chen Wu and Ming Yan. Learning deep semantic model for code search using codesearchnet corpus,
 683 2022. URL <https://arxiv.org/abs/2201.11313>.

684

685 Di Wu, Wasi Uddin Ahmad, Dejiao Zhang, Murali Krishna Ramanathan, and Xiaofei Ma. Repoformer:
 686 Selective retrieval for repository-level code completion. *arXiv preprint arXiv:2403.10059*, 2024.

687

688 Zhou Yang, Jieke Shi, Junda He, and David Lo. Natural attack for pre-trained models of code. In
 689 *Proceedings of the 44th International Conference on Software Engineering*, pages 1482–1493,
 690 2022.

691

692 Kaichun Yao, Hao Wang, Chuan Qin, Hengshu Zhu, Yanjun Wu, and Libo Zhang. Carl: Unsupervised
 693 code-based adversarial attacks for programming language models via reinforcement learning. *ACM*
 694 *Transactions on Software Engineering and Methodology*, 34(1):1–32, 2024.

695

696 Noam Yefet, Uri Alon, and Eran Yahav. Adversarial examples for models of code. *Proceedings of*
 697 *the ACM on Programming Languages*, 4(OOPSLA):1–30, 2020.

698

699 Huangzhao Zhang, Zhuo Li, Ge Li, Lei Ma, Yang Liu, and Zhi Jin. Generating adversarial examples
 700 for holding robustness of source code processing models. *Proceedings of the AAAI Conference*
 701 *on Artificial Intelligence*, 34(01):1169–1176, Apr. 2020a. doi: 10.1609/aaai.v34i01.5469. URL
 702 <https://ojs.aaai.org/index.php/AAAI/article/view/5469>.

703

704 Huangzhao Zhang, Shuai Lu, Zhuo Li, Zhi Jin, Lei Ma, Yang Liu, and Ge Li. Codebert-attack:
 705 Adversarial attack against source code deep learning models via pre-trained model. *Journal of*
 706 *Software: Evolution and Process*, 36(3):e2571, 2024.

702 Wei Emma Zhang, Quan Z. Sheng, Ahoud Alhazmi, and Chenliang Li. Adversarial attacks on
703 deep-learning models in natural language processing: A survey. *ACM Trans. Intell. Syst. Technol.*,
704 11(3), April 2020b. ISSN 2157-6904. doi: 10.1145/3374217. URL <https://doi.org/10.1145/3374217>.

705

706 Penghao Zhao, Hailin Zhang, Qinhan Yu, Zhengren Wang, Yunteng Geng, Fangcheng Fu, Ling Yang,
707 Wentao Zhang, Jie Jiang, and Bin Cui. Retrieval-augmented generation for ai-generated content: A
708 survey. *arXiv preprint arXiv:2402.19473*, 2024.

709

710 Qinkai Zheng, Xiao Xia, Xu Zou, Yuxiao Dong, Shan Wang, Yufei Xue, Lei Shen, Zihan Wang, Andi
711 Wang, Yang Li, Teng Su, Zhilin Yang, and Jie Tang. Codegeex: A pre-trained model for code
712 generation with multilingual benchmarking on humaneval-x. In *Proceedings of the 29th ACM*
713 *SIGKDD Conference on Knowledge Discovery and Data Mining*, KDD '23, page 5673–5684, New
714 York, NY, USA, 2023. Association for Computing Machinery. ISBN 9798400701030.

715 Yu Zhou, Xiaoqing Zhang, Juanjuan Shen, Tingting Han, Taolue Chen, and Harald Gall. Adversarial
716 robustness of deep code comment generation. *ACM Transactions on Software Engineering and*
717 *Methodology (TOSEM)*, 31(4):1–30, 2022.

718

719

720

721

722

723

724

725

726

727

728

729

730

731

732

733

734

735

736

737

738

739

740

741

742

743

744

745

746

747

748

749

750

751

752

753

754

755

756 **A USE OF LLMs**
757758 We detail our use of Large Language Models (LLMs) below:
759760 • **Experimental Application:** The `gpt-4o` model was utilized as a component of the
761 Retrieval-Augmented Generation (RAG) pipeline, as presented in Section 4.5. This was the
762 only application of LLMs in this paper.
763 • **Writing Assistance:** We also employed LLMs to aid in improving the grammar, clarity, and
764 phrasing of the draft during the writing process.
765766 **B LIMITATION**
767768 This study has several limitations. Firstly, our presented attacks exclusively target *(query, code)*
769 pairs. While our gradient-based methodology could potentially modify a code snippet to increase its
770 similarity with multiple queries concurrently (i.e., a *(query_list, code)* input format), such experiments
771 were not conducted due to time constraints.772 Also, although we demonstrated the transferability of adversarial attacks across various code embed-
773 ding models, we have not identified the underlying reasons for this phenomenon. We hypothesize that
774 shared pretraining data among these models contributes to transferability; however, the number of
775 models tested in this work with publicly available pretraining data was insufficient to draw definitive
776 conclusions.
777778 **C COMPUTE RESOURCE**
779780 The experiments described in this paper were conducted on a server equipped with an AMD EPYC
781 Milan 7643 48-Core CPU (@2.30GHz), 1TB of RAM, and an NVIDIA L40 ADA 48GB GPU. We
782 used a batch size of 10 *(query, code)* pairs for attacks on CodeT5+ and 4 pairs for attacks on OASIS.
783 We observed that larger batch sizes did not further reduce the runtime. The time and GPU memory
784 spent on the experiments are reported in Table 10.785 Table 10: Compute resource used in the experiments for generating 10,000 adversarial examples.
786787

Attack Model	Total Time	GPU Time (Gradient Calc.)	CPU Time (Parsing & Token Search)	GPU Memory	Token Search Space
CodeT5+ (110M)	8 hours	~6.8 hours (85%)	~1.2 hours (15%)	7GB	15.1k
OASIS (1.5B)	12 hours	~10.6 hours (88%)	~1.4 hours (12%)	26GB	36.7k

793 **D MODEL & DATASET LICENSE**
794795 • **CodeT5+:** BSD 3-Clause License ²
796 • **OASIS:** MIT License³
797 • **Nomic-emb-code:** Apache-2.0 ⁴
798 • **Voyage-code-3:** Unclear, but we do not include any embeddings from voyage-code-3 in our
800 codebase.
801 • **CosQA:** Apache-2.0⁵ (we use CosQA from COIR)
802 • **CLARC:** CC-BY-SA 4.0: ⁶
803 • **HumanEval-X:** Apache-2.0⁷804 ²<https://github.com/salesforce/CodeT5?tab=BSD-3-Clause-1-ov-file>805 ³<https://huggingface.co/Kwaipilot/OASIS-code-embedding-1.5B>806 ⁴<https://huggingface.co/nomic-ai/nomic-embed-code>807 ⁵<https://github.com/CoIR-team/coir/blob/main/LICENSE>808 ⁶<https://huggingface.co/datasets/ClarcTeam/CLARC>809 ⁷<https://huggingface.co/datasets/THUDM/humaneval-x>

810 E IMPLEMENTATION DETAILS
811812
813 E.1 DETAILED CONSTRAINTS
814815 In the adversarial attack, we focus on replacements of the identifier tokens. More specifically, we
816 replace the tokens that include part of function, variable, macro, and module names in the code text.
817 Formally, let the original code text be tokenized as $\{C_{t_i}\}_{i=1}^n$, and the code text after replacement be
818 tokenized as $\{C'_{t_i}\}_{i=1}^n$. For any two strings A and B , let $\text{LCS}(A, B)$ denote their longest common
819 substring, and let $\text{Remove}(A, B)$ denote the remaining string after removing string B from string A .
820 We introduce two additional constraints during the replacement:821 **Identifier Consistency** If C_{t_i} and C_{t_j} are tokens from different occurrences of the same identifier in
822 the code, then:

823
824
$$\text{Remove}(C'_{t_i}, \text{LCS}(C'_{t_i}, C'_{t_j})) = \text{Remove}(C_{t_i}, \text{LCS}(C_{t_i}, C_{t_j})),$$

825
826

827
828
$$\text{Remove}(C'_{t_j}, \text{LCS}(C'_{t_i}, C'_{t_j})) = \text{Remove}(C_{t_j}, \text{LCS}(C_{t_i}, C_{t_j})).$$

829
830

831 **No Duplicate Replacement** If C_{t_i}, C_{t_j} are tokens from occurrences of one identifier, and C_{t_p}, C_{t_q}
832 are tokens from occurrences of a *different* identifier, then:

833
834
$$\text{LCS}(C'_{t_i}, C'_{t_j}) \neq \text{LCS}(C'_{t_p}, C'_{t_q}).$$

835
836

837 These constraints ensure the code’s AST structure remains identical, thereby preserving semantic
838 consistency between the original and attacked versions of the code. To satisfy the constraints, we
839 employ the Hungarian Algorithm (Kuhn, 1955) to match original identifier tokens with their optimal
840 replacements.841 Let V denote the tokenizer’s vocabulary and $S \subseteq V$ be the set of distinct tokens in the identifiers
842 in the code snippet. For each original token $s_i \in S$, we define an influence function $f_{s_i} : V \rightarrow \mathbb{R}$
843 derived from gradient information. This function, $f_{s_i}(v)$, quantifies the *influence* when s_i is replaced
844 by v .845 The goal is to find a set of matching $\{s_i, v_i\}$ that maximizes the total influence, subject to the
846 constraint that each substitute token v_i must be unique. This can be formulated as the following
847 optimization problem:

848
849
$$\underset{\{v_i\}}{\text{maximize}} \quad \sum_i f_{s_i}(v_i)$$

850
851

852
853
$$\text{subject to} \quad v_i \in V, \quad \text{and} \quad v_i \neq v_j \quad \forall i \neq j.$$

854
855

856
857
858
859
860
861
862
863 The solution to this optimization problem is provided by Algorithm 1

864 **Algorithm 1** Optimal Token Substitution

865

866 **Require:** Set of original tokens $S = \{s_1, \dots, s_m\}$, a vocabulary of candidate tokens V , and an
867 influence function $f_{s_i}(v)$.

868 **Ensure:** An optimal assignment map $M : S \rightarrow V$ and the maximum total influence I_{total} .

869 1: **procedure** FINDBESTMATCHING(S, V, f)

870 2: Let $C \subseteq V$ be the set of candidate tokens where $|C| = n$.

871 3: % Convert the problem to a minimum cost formulation.

872 4: $I_{\text{max}} \leftarrow \max_{s_i, v_j} f_{s_i}(v_j)$.

873 5: Create an $m \times n$ cost matrix \mathbf{W} where $\mathbf{W}_{ij} \leftarrow I_{\text{max}} - f_{s_i}(v_j)$.

874 6: % Solve the assignment problem with the Hungarian Algorithm

875 7: Pairs \leftarrow HungarianAlgorithm(\mathbf{W})

876 8: % Construct the final mapping from the resulting pairs.

877 9: Initialize $M \leftarrow \emptyset$ and $I_{\text{total}} \leftarrow 0$.

878 10: **for** each pair (r, k) in Pairs **do**

879 11: $s_{\text{assigned}} \leftarrow S[r]$, $v_{\text{assigned}} \leftarrow C[k]$

880 12: $M[s_{\text{assigned}}] \leftarrow v_{\text{assigned}}$

881 13: $I_{\text{total}} \leftarrow I_{\text{total}} + f_{s_{\text{assigned}}}(v_{\text{assigned}})$

882 14: **end for**

883 15: **return** M, I_{total}

884 16: **end procedure**

885

886 17: **procedure** HUNGARIANALGORITHM(\mathbf{W})

887 18: % Construct a flow network and apply Ford-Fulkerson for the max flow.

888 19: Create a source S and a sink T . Let m, n be the dimensions of \mathbf{W} .

889 20: **for** $i \leftarrow 1$ to m **do** % Nodes for original tokens

890 21: Create node u_i and add edge $S \rightarrow u_i$ with capacity 1, cost 0.

891 22: **end for**

892 23: **for** $j \leftarrow 1$ to n **do** % Nodes for candidate tokens

893 24: Create node w_j and add edge $w_j \rightarrow T$ with capacity 1, cost 0.

894 25: **end for**

895 26: **for** $i \leftarrow 1$ to m **do** % Edges representing potential assignments

896 27: **for** $j \leftarrow 1$ to n **do**

897 28: Add edge $u_i \rightarrow w_j$ with capacity 1 and cost \mathbf{W}_{ij} .

898 29: **end for**

899 30: **end for**

900 31: Initialize flow $F \leftarrow 0$. Let G_f be the residual graph.

901 32: **while** $F < m$ **do**

902 33: Find the shortest path from S to T in G_f using edge costs as weights.

903 34: **if** no path exists **then**

904 35: **break**

905 36: **end if**

906 37: Let P be the shortest path found.

907 38: Augment 1 unit of flow along path P .

908 39: Update the residual graph G_f for the path P .

909 40: $F \leftarrow F + 1$.

910 41: **end while**

911 42: % Convert the max flow to assignment.

912 43: Initialize an empty set of pairs Pairs.

913 44: **for** each edge $u_i \rightarrow w_j$ that has a flow of 1 **do**

914 45: Add the index pair (i, j) to Pairs.

915 46: **end for**

916 47: **return** Pairs

917 48: **end procedure**

918 E.2 SEARCH SPACE
919

920 For each token position, we need to go over at most V optional tokens to find the optimal token that
921 maximizes $\delta_{(i, t_x)}$, where V is the vocabulary size of the neural code search model. In practice, due
922 to the constraint on the identifier of programming languages, only about 30-40% of the vocabularies
923 are valid tokens to replace the original identifiers.

924 E.3 SPECIFICATION
925

926 The initial step of our adversarial attack involves parsing the input code snippet to locate identifiers
927 suitable for modification. We employ language-specific AST parsers: Python’s built-in `ast` library,
928 `clang` for C++, and `tree-sitter` for Java, JavaScript, and Go. These same parsers are applied
929 again after the adversarial modifications to ensure the modified code snippet remains syntactically
930 identical.

931 When targeting CodeT5+, we restricted this search space to tokens composed solely of alphanumeric
932 characters and spaces. For OASIS, however, the significantly larger vocabulary leads to a more
933 complex situation: tokens representing an identifier may sometimes include a preceding operator. For
934 example, within a code snippet, one occurrence of a variable `x` might correspond to the token `_x`,
935 while another corresponds to `+x`. In such scenarios, when searching for a replacement variable `y`, we
936 specifically look for candidate tokens that maintain this structure—namely, `_y` and `+y` respectively—
937 and select the one that maximizes the influence. Consequently, the search space for OASIS also
938 includes tokens structured as an operator followed by alphanumeric characters and spaces.

939
940 F SUPPLEMENTARY EXPERIMENTAL RESULTS
941942 F.1 DISTRIBUTION OF CODE SIMILARITY CHANGES
943

944 Please refer to Figure 2 for the distribution of the similarity change on CosQA and CLARC.
945

946 F.2 “DENSITY” OF THE EMBEDDING VECTORS FROM DIFFERENT MODELS.
947

948 Table 11 shows the average similarity scores for queries against both their ground truth code and
949 irrelevant code. Notably, the gap between these ground truth and irrelevant similarities is significantly
950 larger on the CLARC dataset than on CosQA for OASIS and Nomic-emb-code.

951 Table 11: Average Similarity Scores and Gaps for Different Models on CosQA and CLARC Datasets
952

954 Dataset	955 Model	956 Avg. Sim between Query and GroundTruth Code	956 Avg. Sim between Query and Irrelevant Code	956 Gap
957 CosQA	CodeT5+	54.15	20.60	33.55
	OASIS	68.53	47.13	21.40
	Nomic-emb-code	41.77	1.95	39.82
	voyage-code-3	71.43	37.83	33.60
961 CLARC	CodeT5+	52.91	25.80	27.11
	OASIS	85.80	54.61	31.19
	Nomic-emb-code	55.71	7.44	48.27
	voyage-code-3	73.93	40.08	33.85

966 F.3 APPLICATION OF THE ADVERSARIAL ATTACK ON CLARC
968

969 Here, we evaluated retrieval metrics on the CLARC dataset before and after the application of
970 adversarial attacks generated using CodeT5+. The performance degradation on CLARC was less
971 significant than that observed on the CosQA dataset. This disparity stemmed mainly from a wider
inherent gap within CLARC: the difference between a query’s similarity to its correct ground truth

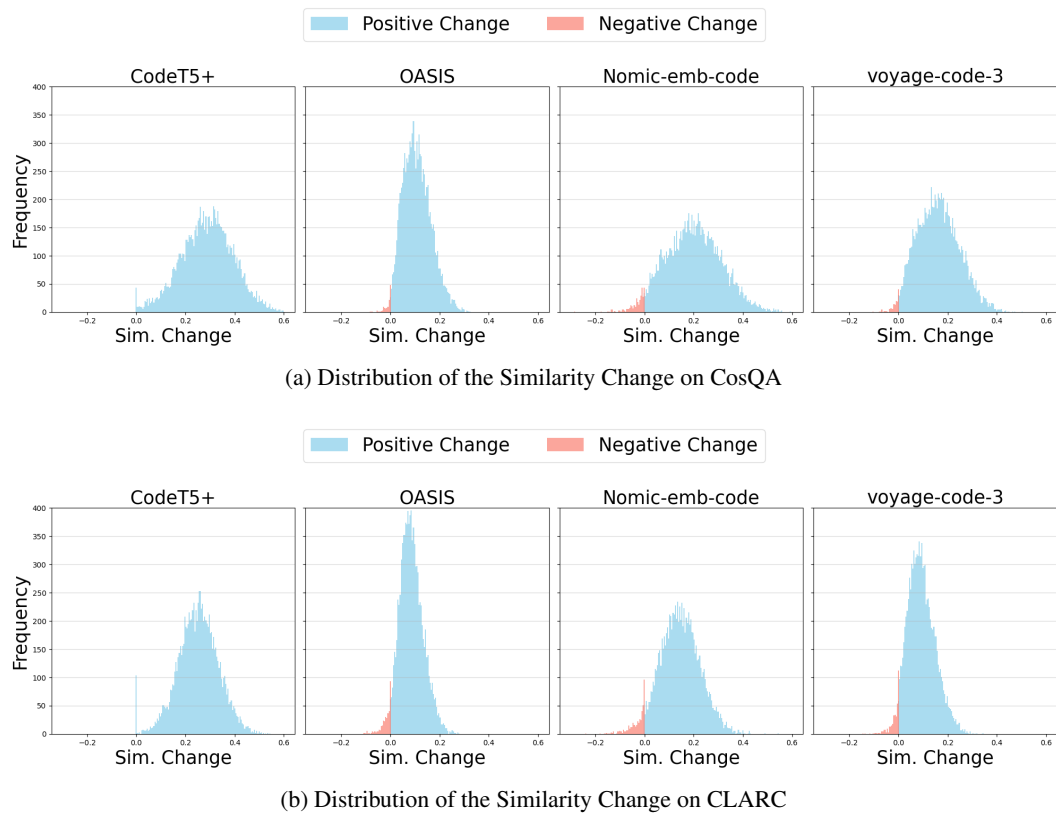


Figure 2: Distribution of Code Similarity Changes. The Attack Model is CodeT5+, and the Eval Models are labeled at the top of each subplot.

code and its similarity to other arbitrary code snippets was larger as illustrated in Table 11. Although the adversarial attack yielded comparable query-code similarity improvements in both datasets, CLARC’s substantial initial gap presents a greater challenge for elevating an adversarial example’s similarity score above that of the ground truth. Consequently, as the evaluation metrics are determined by the rank of the ground truth code, the adversarial attack is less impactful on the retrieval metrics in CLARC.

Table 12: Code Search Metric Change Caused by Adversarial Attack (Data from Screenshot)

Model Name	Setting	NDCG	R@1	R@5	R@10	R@20	MRR
CodeT5	Original	64.54	47.34	74.14	82.51	89.54	58.84
	Adversarial	13.93	5.89	15.59	25.67	36.50	10.42
	Δ	50.61	41.45	58.55	56.84	53.04	48.42
OASIS	Original	89.08	79.85	94.11	96.77	98.48	86.54
	Adversarial	87.44	80.42	91.06	93.54	96.77	85.43
	Δ	1.64	-0.57	3.05	3.23	1.71	1.11
Nomic-emb-code	Original	88.61	80.04	94.11	95.82	96.96	86.23
	Adversarial	85.65	77.95	90.30	92.21	94.11	83.49
	Δ	2.96	2.09	3.81	3.61	2.85	2.74
voyage-code-3	Original	88.96	80.99	94.30	95.06	97.53	86.90
	Adversarial	85.30	76.62	91.06	92.21	95.25	82.98
	Δ	3.66	4.37	3.24	2.85	2.28	3.92

1026

F.4 DETAILS ABOUT METRICS

1027

1028

Correlation Metrics

1029

1030

1031

1032

1033

1034

1035

1036

1037

1038

1039

- **Precision:** The expected conditional probability that an adversarial example induces a positive similarity change on the Eval Model, given that it induced a positive change on the Attack Model.
- **Pearson Correlation Coefficient (r):** Measures the linear correlation between the numerical values of the similarity changes observed on the Attack and Eval Models.
- **Spearman’s Rank Correlation Coefficient (ρ):** Measures the monotonic correlation, assessing how well the rank order of similarity changes is preserved between the Attack and Eval Models.

Retrieval Metrics

1040

1041

1042

1043

1044

1045

1046

1047

1048

1049

1050

1051

1052

1053

- **Recall@k (R@k):** The proportion of queries for which the correct code snippet is found within the top-k ranked results returned by the model. Since each query in the CosQA and CLARC datasets has exactly one ground-truth matching code snippet, R@k specifically measures the percentage of queries where this single correct snippet appears among the top k candidates.
- **Normalized Discounted Cumulative Gain (NDCG):** A metric for evaluating the quality of a ranked list. It assigns higher scores when relevant items are placed higher in the ranking, applying a logarithmic discount based on position. The score is normalized against the ideal ranking, resulting in a value between 0 and 1.
- **Mean Reciprocal Rank (MRR):** The average of the reciprocal ranks across all queries in the test set. For a single query, the reciprocal rank is the inverse of the rank position (1/rank) of the ground truth code snippet.

F.5 APPLICATION ON BENCHMARK

1054

1055

Table 13: Model Performance Under Different Attack Percentages

Model Name	% of Corpus Attacked	MRR Difference	NDCG Difference	R@1 Difference	R@5 Difference	R@10 Difference	R@20 Difference
CodeT5+	1%	36.88	29.18	45.40	27.80	3.40	1.00
	2%	48.15	42.87	50.40	50.40	23.60	1.80
	5%	58.60	58.48	55.60	61.60	57.40	37.40
	10%	62.27	63.33	56.80	70.00	65.80	58.80
OASIS	1%	13.08	17.32	18.60	5.00	1.60	0.20
	2%	20.07	16.51	25.20	10.00	5.20	0.40
	5%	32.39	28.44	37.00	24.60	15.40	6.00
	10%	39.64	36.42	42.00	36.20	25.40	14.60
NOMIC	1%	14.31	11.28	19.00	5.60	1.60	0.40
	2%	21.52	17.40	27.40	12.00	4.00	1.00
	5%	32.32	28.64	36.80	25.00	16.40	5.40
	10%	40.01	36.66	43.40	34.80	25.40	15.80
voyage-code-3	1%	11.11	8.53	15.80	3.20	0.40	0.00
	2%	16.90	13.18	24.00	5.20	1.40	0.20
	5%	27.43	23.02	33.00	19.00	8.40	2.60
	10%	36.09	31.92	41.40	27.00	18.20	8.60

1074

1075

1076

1077

We evaluated the impact of poisoning 1%, 2%, and 5% of the corpus, in addition to the original 10% setting in Table 13. For context, with a total corpus size of 500 snippets, a 1% attack corresponds to manipulating just 5 code snippets.

1078

1079

We find the attack is highly effective even at minimal levels. A mere 1% poisoning of the corpus causes substantial performance degradation. For example, Recall@1 drops by 45.4% in the white-box setting (CodeT5+) and 15.8% in the black-box setting (Voyage-code-3).

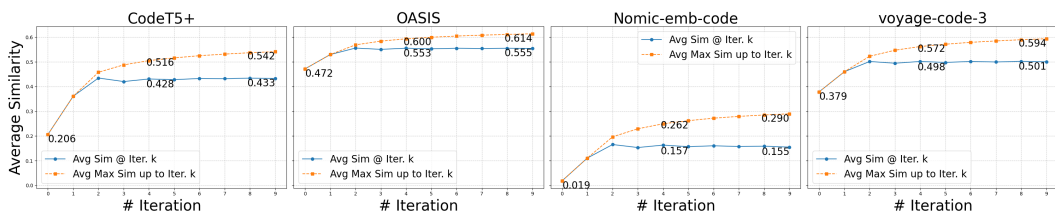
1080 As the attack percentage increases, the negative impact becomes more severe, with the degradation
 1081 at a 5% attack rate already approaching the levels of the 10% scenario from our draft. These
 1082 results confirm that our attack does not rely on an unrealistic number of poisoned examples and can
 1083 effectively compromise code retrieval systems even when a small fraction of the corpus is malicious.
 1084

1085 F.6 ABLATION STUDIES

1087 We conduct ablation studies to evaluate the contribution of specific components within our attack
 1088 method.

1089
 1090 **Attack Code Selection** Our default strategy selects the adversarial code that achieves the highest
 1091 similarity to the query across all iterations of the attack process. In this ablation, we compare this
 1092 approach with an alternative that selects the adversarial code directly from a fixed iteration k in order
 1093 to justify the necessity of our adversarial code selection strategy.

1094 We evaluated both strategies using the 10,000 sampled $(query, code)$ pairs from CosQA for 10
 1095 iterations. Figure 3 plots the average query-code similarity at each iteration k for both approaches.
 1096 The alternative approach, which selects the code at iteration k (blue solid line), shows diminishing
 1097 returns, as the average similarity plateaus and fluctuates after three iterations. In contrast, selecting
 1098 the code with the maximum similarity observed up to iteration k (orange dashed line) allows the
 1099 average similarity to increase monotonically throughout the process, achieving much higher final
 1100 similarities. The comparison confirms the benefit of retaining the highest-scoring code variant across
 1101 all iterations rather than only considering the final iteration’s output.



1100 Figure 3: Avg. Similarity Change between Pairs Sampled from CosQA based on CodeT5+ Attack.
 1101 Picking the code with the max similarity up to iteration k leads to higher similarity changes.

1102
 1103 **Iteration Limit** Our standard adversarial attack protocol employs 5 iterations. However, Figure 3
 1104 (orange dashed lines) reveals that the average query-code similarity, using our optimal strategy of
 1105 selecting the best code up to iteration k , continues to increase beyond 5 iterations on the CosQA
 1106 dataset across different evaluation models. Our decision to limit the process to 5 iterations is a result
 1107 of the practical trade-off between computational cost and the magnitude of similarity improvement.
 1108 Extending the attack from 5 to 10 iterations, for instance, would approximately double the runtime
 1109 while yielding only marginal further gains in average similarity (observed to be less than 0.03 across
 1110 all models between iterations 5 and 10, based on Figure 3). Considering the substantial effectiveness
 1111 already demonstrated in our main experiments, we think 5 iterations are enough for most cases.
 1112 Nevertheless, these results suggest that performing additional iterations could be beneficial, yielding
 1113 further improvements when computational resources are not a primary constraint.

1124 G EXAMPLES

1125 For more examples, please refer to our GitHub Repository at https://github.com/AdvAttackOnNCC/Code_Search_Adversarial_Attack.

1130 G.1 EXAMPLES FROM DATASETS

1131 G.1.1 CosQA

1132 **Query Example** s3 sync between bucket python

1134

Code Snippet Example

```

1135
1136 def assert_or_raise(stmt: bool, exception: Exception,
1137     *exception_args, **exception_kwargs) -> None:
1138     if not stmt:
1139         raise exception(*exception_args, **exception_kwargs)
1140
1141
```

G.1.2 CLARC

1142

Query **Example** The function takes an unsigned 8-bit integer representing a character as input and returns a string representing that character. If the input is a displayable character, it is directly converted to its string equivalent; otherwise, the function produces a string in which the integer value of the non-printable character is enclosed in angle brackets. The resulting string is returned as the output.

1143

Code Example

1144

1145

1146

1147

1148

1149

1150

1151

1152

1153

1154

1155

1156

1157

1158

1159

1160

1161

1162

1163

1164

1165

1166

1167

1168

1169

1170

1171

1172

1173

1174

1175

G.2 ADVERSARIAL ATTACK EXAMPLES

1176

1177

G.2.1 CosQA

1178

1179

1180

Attacked by CodeT5+ The following example is the adversarial code based on the query and code snippet examples provided in Section G.1.1. The similarity increases by 66.06% from the original code to this adversarial code.

1181

1182

1183

1184

1185

1186

1187

```

def bucketSynchronLossSyncQS( sa: bool, sync: Exception,
                                *lintCachingTM, **ScalingdingsClears) -> None:
    if not sa:
        raise sync(*lintCachingTM, **ScalingdingsClears)
```

Attacked by OASIS The following example is the adversarial code based on the query and code snippet examples provided in Section G.1.1. The similarity increases by 12.97% from the original code to this adversarial code.

```

1188 def testsvisorFileType( SOUR: bool, UIStoryboardSegue: Exception,
1189           *OptionsResolveracos, **_documentobucket) -> None:
1190   if not SOUR:
1191     raise UIStoryboardSegue(*OptionsResolveracos, **_documentobucket)
1192
1193
1194 G.2.2 CLARC
1195
1196 Attacked by CodeT5+ The following example is the adversarial code based on the query and code
1197 snippet examples provided in Section G.1.2. The similarity increases by 54.24% from the original
1198 code to this adversarial code.

```

```

1198   asStringCharCodeDisplaysrepresentationFarvancetextarea
1199   float
1200     TemporaryBGCWigClassAttributeharitutdowntreat(float character);
1201     asStringCharCodeDisplaysrepresentationFarvancetextarea
1202   float
1203     TemporaryBGCWigClassAttributeharitutdowntreat(float character) {
1204       float Room, combo, HT, pil, ign, bw;
1205
1206       Room = 1.70158f;
1207       ign = Room * 1.525f;
1208       bw = 0.5f;
1209       HT = character / 0.5f;
1210
1211       if ( HT < 1.0f) {
1212         combo = ( ign + 1) * HT - ign;
1213         pil = HT * HT * combo;
1214         return bw * pil;
1215       }
1216
1217       HT -= 2.0f;
1218       combo = ( ign + 1.0f) * HT + ign;
1219       pil = ( HT * HT * combo) + 2;
1220
1221       return bw * pil;
1222     }
1223
1224
1225
1226 Attacked by OASIS The following example is the adversarial code based on the query and code
1227 snippet examples provided in Section G.1.2. The similarity increases by 28.94% from the original
1228 code to this adversarial code.

```

```

1224 VerbFRFRINGcrediblexr
1225   float
1226     ASCIIilityMOSTpyxuctDISPLAYegtereburgInInspectorDisplay(float char);
1227     VerbFRFRINGcrediblexr
1228   float
1229     ASCIIilityMOSTpyxuctDISPLAYegtereburgInInspectorDisplay(float char) {
1230       float UNC, c, ostr, HSV, UTF, SENT;
1231
1232       UNC = 1.70158f;
1233       UTF = UNC * 1.525f;
1234       SENT = 0.5f;
1235       ostr = char / 0.5f;
1236
1237       if ( ostr < 1.0f) {
1238         c = ( UTF + 1) * ostr - UTF;
1239         HSV = ostr * ostr * c;
1240         return SENT * HSV;
1241       }
1242
1243       ostr -= 2.0f;
1244       c = ( UTF + 1.0f) * ostr + UTF;
1245       HSV = ( ostr * ostr * c) + 2;

```

```
1242
1243     return SENT * HSV;
1244 }
1245
1246
1247
1248
1249
1250
1251
1252
1253
1254
1255
1256
1257
1258
1259
1260
1261
1262
1263
1264
1265
1266
1267
1268
1269
1270
1271
1272
1273
1274
1275
1276
1277
1278
1279
1280
1281
1282
1283
1284
1285
1286
1287
1288
1289
1290
1291
1292
1293
1294
1295
```